International Journal of GEOMATE, June 2023, Vol. 24, Issue 106, pp.69-76
ISSN: 2186-2982 (P), 2186-2990 (O), Japan, DOI: https://doi.org/10.21660/2023.106.g12209
Geotechnique, Construction Materials and Environment

NUMERICAL STUDY OF A HYBRID COUNTERMEASURE FOR RIVER EMBANKMENT IN ACTUAL FIELD CASE

*Kakuta Fujiwara[1]and Enayat Mallyar[1]

[1] Dept. of Civil Eng., Tokai University, Japan

*Corresponding Author, Received: 06 Aug. 2022, Revised: 31 Jan. 2023, Accepted: 19 March 2023

ABSTRACT: In this study, a hybrid countermeasure for river embankments is proposed consisting of a wall of sheet-piles installed on one side of the toe of embankment and partial floating sheet-piles (PFS) installed on the other. Previous studies show that the PFS method is effective against embankment settlement caused by liquefaction of loose sand and consolidation of soft clay. However, such previous studies were carried out on simple model cases, and hybrid countermeasures on actual embankments have not been thoroughly studied. Therefore, the authors have performed numerical analyses to verify the effectiveness of the hybrid countermeasure applied to actual field conditions with an earthquake motion occurred in the past. It was concluded that the settlement of embankment was reduced by the hybrid countermeasure even in the actual field case. Additionally, authors obtained fundamental data for making a design method, that is the maximum bending stress among the different lengths of the sheet-piles after consolidation.

Keywords: Numerical analysis, Liquefaction, Countermeasure, PFS, Three-dimension

1. INTRODUCTION

Loose sand layers along river embankments are continuously damaged and settled due to liquefaction caused by earthquakes. As a conventional countermeasure, sheet-piles are installed at both toes of the embankment to potentially prevent damage to the embankment as well as settlement along the embankment, according to Fujiwara et al [1], [2]. There are several examples of river embankments in Japan that demonstrate the effectiveness of sheet-piles against settlement due to earthquakes (Fig. 1(a)).

However, a layer of soft clay near the river embankment settles due to consolidation caused by the weight of the embankment. Otani [3] studied the partial floating sheet-pile (PFS), which consists of partially floating sheet-piles and end-bearing sheet-piles (Fig. 2), applied to one side of the toe of the embankment in a residential area (Fig. 1 (b)).

Nowadays, a "hybrid countermeasure" (a term coined by the authors in this paper) is in use (Fig.1 (c)), where an embankment having clay and sand layers has sheet-piles installed in river areas and the PFS installed in residential areas along both toes of the embankment. Yamamoto et al [4] investigated certain examples where the damage to a river embankment, due to consolidation and liquefaction during long-term including an earth-quake event was reduced through the use of hybrid countermeasures. Such hybrid countermeasures could be effective against soil deformation due to liquefaction and consolidation. However, the behavior and effectiveness of these hybrid countermeasures are not fully understood.

As a first step, Fujiwara et al [5] carried out numerical analysis to verify the effectiveness of the PFS method for a river embankment under liquefaction. They concluded that the PFS could inhibit settlement of the embankment under liquefaction. Furthermore, the relationship between the parameters of the sheet-pile, such as the distance between the end-bearing sheet-piles and the length of the floating sheet-piles, as well as their effectiveness against settlement was verified.

However, these analyses were carried out under several simple assumptions as follows:

· Vertical load was applied to the surface ground instead of modelling of an embankment.

· The ground had only two sand layers.

· A sinusoidal wave with enormous acceleration was given as an input.

· Bending stress of sheet-piles were not discussed for making a design method

2. THE RESEARCH SIGNIFICANCE

From the introduction, the authors carried out numerical analyses to investigate the effectiveness of the hybrid countermeasure against settlement in an actual field case to improve the previous numerical model. Additionally, the authors discussed the bending stress of the sheet-piles in the PFS for the purpose of designing this countermeasure. One of the effective countermeasures for an embankment against consolidation and liquefaction can be established through the above study.

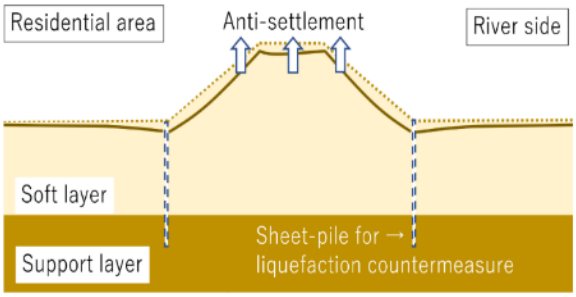

(a) Sheet-piles as a liquefaction countermeasure

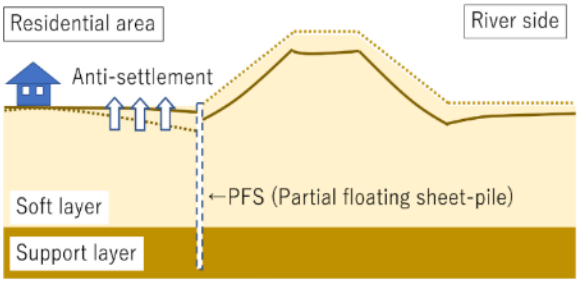

(b) PFS to prevent settlement by consolidation

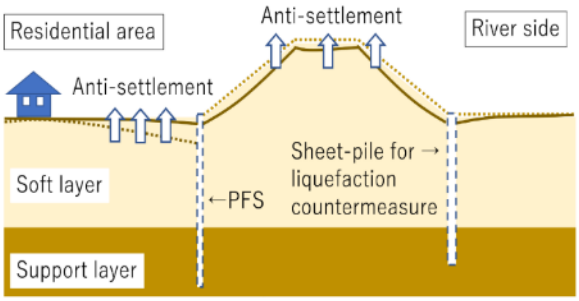

(c) Hybrid countermeasure

Fig. 1 Countermeasures for the river embankment

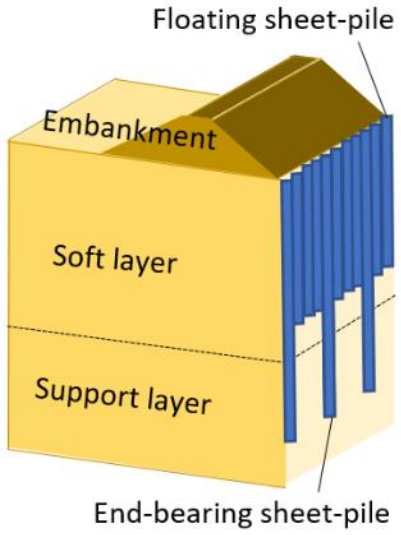

Fig. 2 The PFS structure

3. NUMERICAL CONDITION

The numerical analyses were conducted using LIQCA3D20. The LIQCA has been used in numerical analyses of the behaviours of embankments, retaining walls and buildings, as well as in other constructions under liquefaction.

The target embankment is constructed on six horizontal layers of ground shown as Fig.3. The water level was 1.5m under surface ground. The width and depth of this model was relatively small for reduction of calculation time. Model size should be considered in the future. To perform the numerical analysis, parameters such as dimensions, soil parameters, and countermeasures needed to be specified. The following sub-sections describe the ground condition and these parameters and their corresponding values.

3.1 Soils

The soil parameters used in the numerical model are shown in Table 1. Some pieces of information (soil species, N value, water level) could be gained by a ground survey. Detail information (stress-strain relationship, liquefaction curve, consolidation test result, and so on) were not gained. Therefore, these parameter values were inferred and determined from the survey results referring to the manual of LIQCA by Liquefaction Geo Research Institute [6] and the academic paper by Fujiwara et al [7].

The embankment and basement (Dg) are modeled as elastic-perfectly plastic models. The sand layers (As1 and As2) were modeled as elasto-plastic models created by Oka et al [8], which is often used to model a loose sand layer. This model represents sand behavior resulting from an increase in excess pore water pressure which causes motion, making the sand soft, and finally causing liquefaction. An elasto-viscoplastic model proposed by Adachi [9], which can represent an increase in excess pore water pressure by the load, making the clay soft and causing consolidation. Dry and saturation conditions are applied to soil above and under the water level, respectively.

3.2 Countermeasures

The sheet-piles were installed along the toe of the embankment, shown as Fig. 3, in residential area. The PFS has three floating sheet-piles and one end-bearing sheet-pile per one set shown in Fig. 4. The sheet-piles were modeled by cuboid meshes with linear elastic material having no yield. The PFS sheet-piles in the residential area were modeled with a flexural rigidity of 8.0×10^4 kN·m^2 (per unit width of 1 m) and a thickness of 210 mm, such that the flexural rigidity was equivalent to that of a IVw

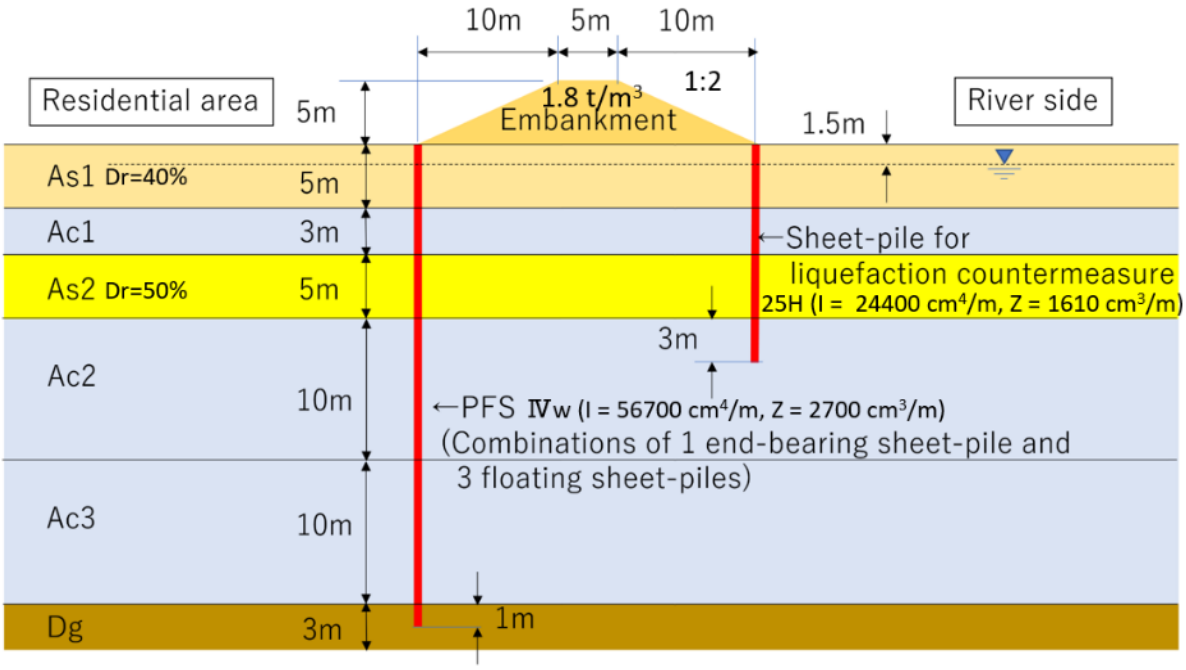

Fig. 3 Target embankment

Table 1 Soil parameters

Layer			Embankment	As1	Ac1	As2	Ac2	Ac3	Dg
Model			Elastic-perfectly plastic	Elasto-plastic	Elasto-viscoplastic	Elasto-plastic	Elasto-viscoplastic	Elasto-viscoplastic	Elastic-perfectly plastic
Density	ρ	t/m^3	1.8	1.8	1.7	1.9	1.7	1.7	2.1
Young's moduls	E_0	kN/m^2	14000	9810	5730	30000	7040	7040	140000
Poisson's ratio	ν		0.33	0.33	0.33	0.33	0.33	0.33	0.33
Cohesion	C	kN/m^2	0	0	20	0	50	70	0
Friction angle	ϕ	degree	30	30	0	30	0	0	40
Coefficient of permeability	k	m/s		1.0×10^{-5}	1.0×10^{-8}	1.0×10^{-5}	1.0×10^{-8}	1.0×10^{-8}	1.0×10^{-4}
Initial void ratio	e_0			0.821	1.25	0.856	1.25	1.25	
Compression index	λ			0.015	0.341	0.018	0.341	0.341	
Swelling index	κ			0.002	0.019	0.0055	0.019	0.019	
	OCR*			1.0	1.0	1.0	1.0	1.0	
Initial elastic shear modulus ratio	G_0/σ'_m			1000	75.2	851	75.2	75.2	
Stress ratio at critical state	M^*_m			0.909	1.24	0.909	1.24	1.24	
Stress ratio at failure	M^*_f			1.122	1.24	1.122	1.24	1.24	
	B^*_0			7000	100	2200	100	100	
Hardening parameter	B^*_1			50	40	30	40	40	
	C_f			2000	10	2000	10	10	
	C_1	1/s			1.0×10^{-5}		1.0×10^{-5}	1.0×10^{-5}	
Viscoplastic parameter	C_2	1/s			3.83×10^{-6}		3.83×10^{-6}	3.83×10^{-6}	
	m'				24.68		24.68	24.68	
Structural parameters	β				3.6		3.6	3.6	
Scalar hardening parameter	A^*_2				5.9		5.9	5.9	
	B^*_2				1.8		1.8	1.8	
Dilentancy parameter	D_0			3		5			
	n			3		1.5			
Reference strain parameter	γ^{P*}			0.02		0.1			
	γ^{E*}			0.01		0.015			

steel sheet-pile, considering corrosion allowance. The sheet-piles on the river side were modeled with a flexural rigidity of 4.0×10^4 kN·m^2 (per unit width of 1 m) and a thickness of 300 mm, such that the flexural rigidity was equivalent to that of a 25H steel sheet-pile, considering corrosion allowance. As the values of flexural rigidity and the section modulus cannot be the same as the actual values of the sheet-piles, the section modulus of the cuboid sheet-piles were higher than the actual value of the sheet-piles. Therefore, the bending stress (discussed herein later) of the cuboid sheet-piles was lower than the actual value of the sheet-piles.

3.3 Numerical Cases

Numerical cases are shown in Table 2. For Case 1, no sheet-piles were set in the numerical model. For Case 2, the target field with the hybrid countermeasure was modeled, as explained herein above. As a further study, the length of the end-bearing sheet-piles was changed for making a design method. For Case 3, the length of the end-bearing sheet-pile was 27 m. For Case 4, the length of the end-bearing sheet-pile was 16 m, which was the same as that of the floating sheet-piles.

3.4 Input Motion

The dynamic analyses were carried out from the results of the initial analyses, using the input motion, which was observed in the Kumamoto Earthquake in 2016 in Japan, as represented by the plot (Fig. 5). The Japan Meteorological Agency provided the data [10]. This wave had a maximum acceleration of 3.24 m/s^2, and a duration of 43 s. The long-term analyses were carried out after shaking, using input data of no acceleration up to t = 3.0E+07 s, which is approximately one year.

3.5 Target Points

The locations of target points D, P1, P2, and P3 (discussed herein later) are selected for discussion indicated in Fig. 6. These points are located in the center of this model. The point D indicates vertical displacement located at top of the embankment, whereas the points P1, P2, and P3 indicate the excess pore water pressure located at 33m, 25m and 13m from bottom of the model, respectively. The displacement boundary conditions are also indicated in Fig. 6.

4. RESULT AND DISCUSSION

Through the analyses results, the deformation of the embankment, water pressure of the ground and bending stress of the sheet-piles are discussed in this chapter.

4.1 Deformation of Ground

The ground deformations for Cases 1 and 2 are shown in Figs. 7 (a) ~ (f). The excess pore water pressure ratios at the end of shaking (t = 43 s.) and at the end of calculation (t = 3.0E+07 s) are colored in Figs. 7 (a), (b) and (c), (d), respectively. The excess pore water pressure ratio means a value that the excess pore water pressure is divided by the initial mean effective stress. Therefore, 1.0 means liquefaction colored in red. The volume strains at the end of calculation (t = 3.0E+07 s) are colored in Figs. 7 (e) and (f).

Table 2 Numerical cases

	The length "L" of the end-bearing sheet-pile
Case 1	no sheet-pile
Case 2	34 m
Case 3	27 m
Case 4	16 m (same as the floating sheet-pile)

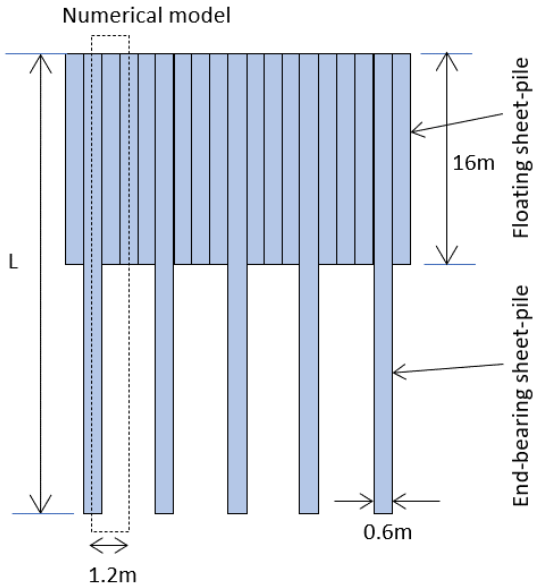

Fig. 4 The PFS structure

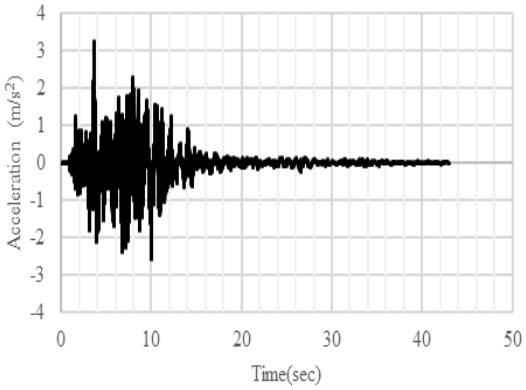

Fig. 5 Input motion

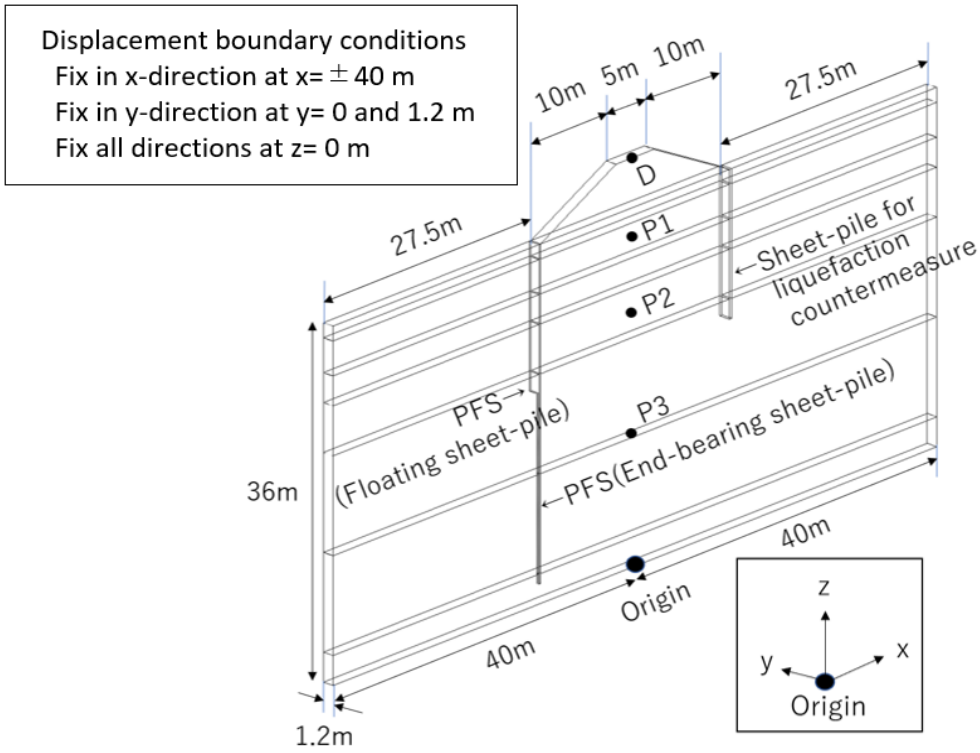

Fig. 6 Model size and target point

Time histories of the settlement at D were shown in Fig. 8. The horizontal displacements of the soil and sheet-piles at the toe of the embankment along z-direction at t = 3.0E+07 s in residential area was shown in Fig. 9. The time histories of the excess pore water pressure at P1, P2, and P3 were shown in Fig. 10 (Case 1).

For Cases 1 and 2, the sand layers were liquified and clay layers were not liquefied in Figs. 7(a) and (b). As time passed in Figs. 7(c) and (d), almost excess pore waters in the sand layers were drained out from the surface ground. On the other hand, the excess pore water pressure under the upper clay layer remained because its permeability was very low. The volume strain in the sand layers was larger than that in the clay layers at t = 3.0E+07 s, shown in Figs. 7(e) and (f). However, the volume strain in the clay layers would continue to increase after t = 3.0E+07 s because the excess pore water pressure remains for a long time.

The liquefied sand layers laterally moved outwards, due to the weight of the embankment. After the shaking, although the void water drained out from the surface (as seen from the data at P1), the excess pore water pressure at P3 increased in the clay layers (Fig. 10). This is because the shear force from the weight of the embankment applied to the clay layers generated the water pressure at P3. Additionally, the permeability of the clay layers is very low. Therefore, the excess pore water pressure layers remained. The settlement of the embankment was 1.33 m at t = 3.0E+07 s and would continue to raise after t = 3.0E+07 s due to the settlement of the clay layers.

For Case 2, the sheet-pies prevented the settlement up to 1.16 m, this was 13% lesser than that in Case 1 at t = 3.0E+07 s shown in Fig. 8. The volume strain near the left sheet-pile of the PFS reduced, which means that the friction of the sheet-piles reduced the ground settlement (Fig. 7(f)). For Cases 3 and 4, the settlements were almost same. In this analysis, the elements of the sheet-pile were connected directly to the soil elements without any joining elements. Therefore, soil didn't pass through between the gap between end-bearing sheet-piles. Accordingly, there was little difference of settlements among Cases 2, 3 and 4 shown in Fig. 8. The behavior of liquefied sand between walls should be discussed by other methods such as a model experiment.

4.2 Bending stress

As a large stress causes yield or failure of the sheet-pile, a discussion about stress of the sheet-piles is essential for making a design method.

Fig 11 shows the bending stress of the end-bearing sheet-pile obtained from Fig. 9 at t = 3.0E+07 s. For Case 2, that is long end-bearing sheet-piles case, the maximum bending stress was generated in the lower layer. For Case 4, that is short end-bearing sheet-piles case, the maximum bending

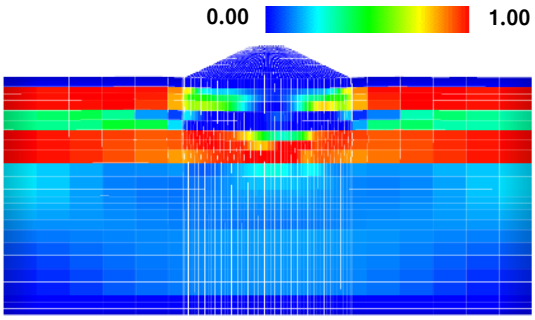

(a) Case 1 (Excess pore water pressure ratio at 43 s.)

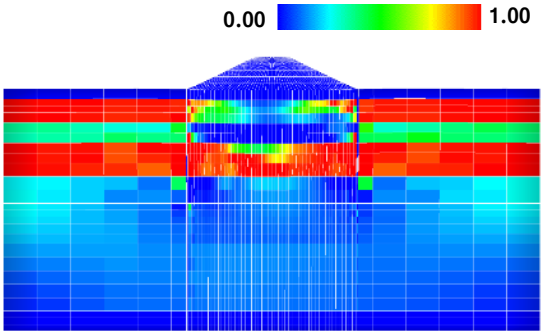

(b) Case 2 (Excess pore water pressure ratio at 43 s.)

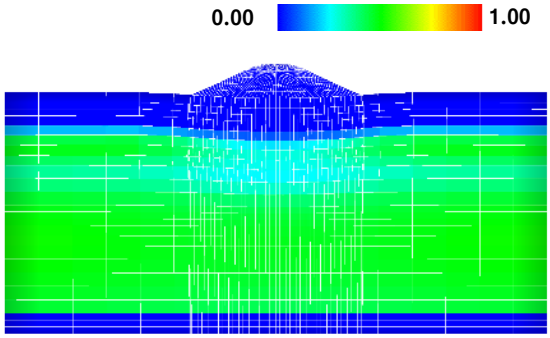

(c) Case 1 (Excess pore water pressure ratio at t = 3.0E+07 s.)

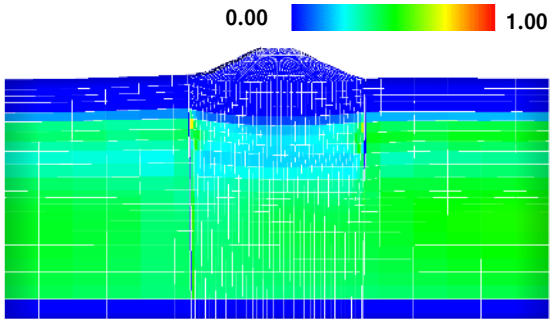

(d) Case 2 (Excess pore water pressure ratio at t = 3.0E+07 s.)

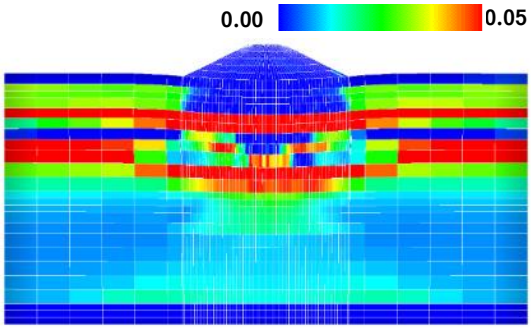

(e) Case 1 (Volume strain at t = 3.0E+07 s.)

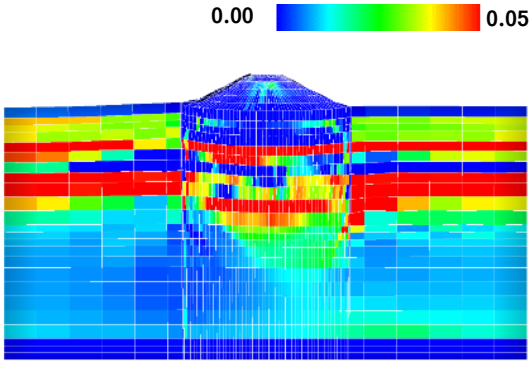

(f) Case 2 (Volume strain at t = 3.0E+07 s.)

Fig. 7 The ground deformation with excess pore water pressure ratio and volume strain

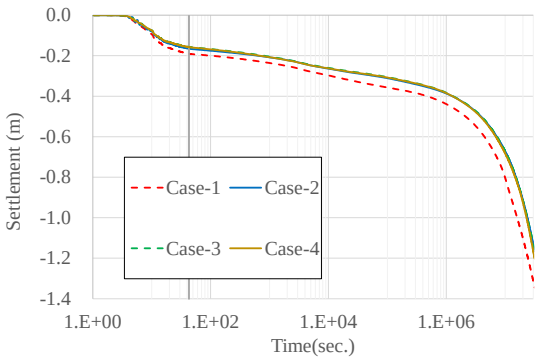

Fig. 8 Time histories for settlement at D

stress was generated in upper layer. For Case 3, the medium result between Cases 2 and 4 was obtained. From Fig. 9, a difference in the displacements for Cases 2, 3 and 4, could be seen near the top of the sheet-pile. The top of the short end-bearing sheet-pile was moved to the right side by the motion of the ground, indicated in Case 1. There were minor differences of bending stress in the clay layers among Cases 2, 3 and 4, which was the same as the result of horizontal displacements. The clear differences along the upper side of the sheet-pile were caused by the deformation of soil, as mentioned earlier in the explanation of horizontal displacement. For Case 4, the lower side of the

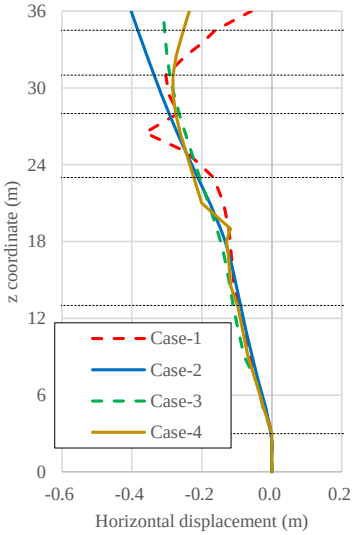

Fig. 9 Horizontal displacement for the PFS sheet-pile in residential area (t = 3.0E+07 s)

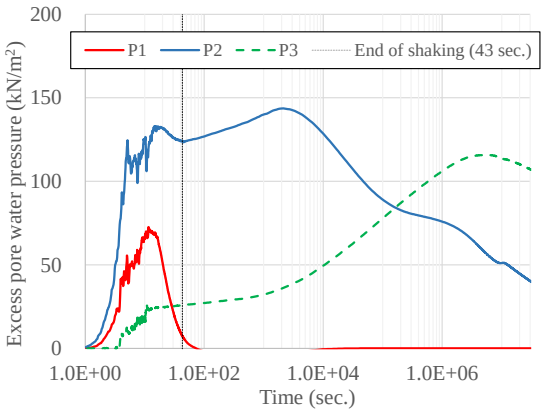

Fig. 10 Time histories for excess pore water pressure at P1, P2 and P3 (Case 1)

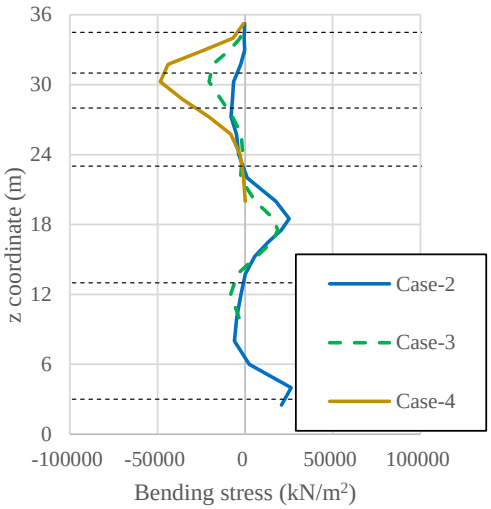

Fig. 11 Bending stress for the sheet-pile in depth direction (t = 3.0E+07 s)

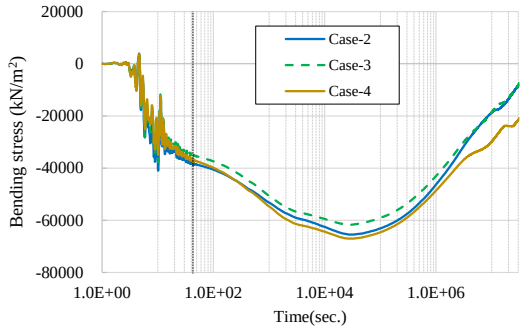

Fig. 12 Time histories for bending stress at z = 30 m

sheet-pile was inclined towards the left side by the deformation of the clay layers and the upper side was pushed to the right side, generating large bending stress around z = 30 m. As the longer the sheet-pile became, the smaller the bending stress became at z = 30 m. Above all, Case 4 had the highest bending stress among Cases 2, 3 and 4.

The time histories of the peak bending stress at z = 30 m are shown in Fig. 12. The bending stress for Cases 2, 3, and 4 were nearly the same during and after shaking. As the excess pore water pressure at P2 and bending stress at z = 30 m are in same layer (As2), these values are strongly correlated, shown in Fig. 10 and Fig. 12. Since all the excess pore water pressure did not dissipate in this analysis, the bending stress would continue to change after t = 3.0E+07 s. The bending stress of the sheet-piles changes for a long time in a condition that the ground includes clay layers.

5. CONCLUSIONS

A hybrid countermeasure for river embankment comprising sheet-piles on the river side and the PFS in the residential area is proposed. Numerical analysis was carried out using LIQCA3D20 to investigate the performance of this countermeasure, applied in the actual field, for a period of one year from an earthquake event.

The following conclusions were reached:

1) The deformation of the embankment was caused by sand liquefaction and clay consolidation. Although the liquefaction dissipated for a short while by the drainage of pore water, the consolidation remained for a long term.

2) One year after the shaking that accompanied the quake, the sheet-piles prevented the settlement by 13% compared to no countermeasure case, even in the actual field case.

3) The behavior of an end-bearing sheet-pile in the PFS was investigated by changing the length of the end-bearing sheet-pile. The maximum bending stress was generated in the sand layers near surface for short end-bearing sheet-piles case.

4) There was little difference of settlements for countermeasure cases among different length of the sheet-piles. This is because soil and sheet-piles were connected directly without joint elements. Therefore, soil didn't pass through between the gap of end-bearing sheet-piles under floating sheet-piles.

5) The model size and target term were limited for the reduction of calculation time in this study. As the deformation would continue after one year, a further analysis will be needed in a future work.

6. ACKNOWLEDGMENT

We are grateful to International Press-in Association TC3 Design WG members (Hidetoshi Nishioka, Hiroaki Akutagawa, Jun Otani, Kiyonobu Kasama, Shinji Taenaka, Shin Oikawa, Yukihiro Ishihara) for helpful discussions.

7. REFERENCES

[1] Fujiwara, K., Koseki, J., Otsushi, K. and Nakayama, H.**,** Study on reinforcement method of levees using steel sheet-piles, Foundation and Soft Ground Engineering Conference, Thu Dau Mot University ICTDMU-1, 2013, pp. 281-289.

[2] Fujiwara, k., Reinforcement method for coastal dyke using double sheet-pile against large earthquake, Doctoral thesis, 2017

[3] Otani, J., A new sheet-pile method for countermeasures against the settlement of embankment on soft ground (Development of PFS Method), IPA News Letter, Vol. 2, Issue 3, 2017, pp. 8-10.

[4] Yamamoto, S., Kasama, K., Ohno, M. and Tanabe, Y., Seismic behavior of the river embankment im-proved with steel sheet piling method, proceedings of the First International Conference on Press-in Engineering, Kochi, 2018, pp. 227-232.

[5] Fujiwara, K., Ogawa, N. and Nakai, K, 3-D numerical analysis of partial floating sheet-pile method as countermeasure for liquefaction, Journal of JSCE, Vol. 9, 2021, pp. 138-147.

[6] Oka, F., Yashima, A., Shibata, T., Kato., M. and Uzuoka, R., FEM-FDM coupled liquefaction analysis of a porous soil using an elasto-plastic model, Applied Scientific Research, Vol. 52, 1994, pp. 209-245.

[7] Fujiwara, K., Ogawa, N. and Nakai, K., Quantitative evaluation of PFS (Partial floating Sheet-pile) method under liquefaction. Geotechnics for Sustainable Infrastructure Development, 2020, pp. 467-472.

[8] Oka, F., Yashima, A., Tateishi, A., Taguchi, Y. and Yamashita, A., A cyclic elasto-plastic constitutive model for sand considering a plastic-strain dependence of the shear modulus, Geotechnique, 1999, Vol. 49(5).

[9] Adachi, T. and Oka, F., Constitutive equations for normally consolidated clay based on elasto viscoplasticity, Journal of Soils and Foundations, Vol. 2, Issue 4, 1982, pp. 57-70.

[10] Japan Meteorological Agency (http://www.data.jma.go.jp/svd/eqev/data/)